J Electroceram (2010) 25:150–158
DOI 10.1007/s10832-010-9606-7

Investigation of top electrode for PZT thick films based MEMS sensors

Christian C. Hindrichsen · Thomas Pedersen · Paw T. Kristiansen · Rasmus Lou-Møller · Karsten Hansen · Erik V. Thomsen

Received: 15 August 2008 / Accepted: 7 April 2010 / Published online: 27 April 2010

Abstract In this work processing of screen printed piezoelectric PZT thick films on silicon substrates is investigated for use in future MEMS devices. E-beam evaporated Al and Pt are patterned on PZT as a top electrode using a lift-off process with a line width down to 3 μm. Three test structures are used to investigate the optimal thickness of the top electrode, the degradation of the piezoelectric properties of the PZT film in absence of a diffusion barrier layer and finally how to fabricate electrical interconnects down the edge of the PZT thick film. The roughness of the PZT is found to have a strong influence on the conductance of the top electrode influencing the optimal top electrode thickness. A 100 nm thick top electrode on the PZT thick film with a surface roughness of 273 nm has a 4.5 times higher resistance compared to a similar wire on a planar SiO_2 surface which has a surface roughness of less than 10 nm. It is found that the piezoelectric properties of the PZT thick film are degraded up to 1,000 μm away from a region of the PZT thick film that is exposed directly to the silicon substrate without a diffusion barrier layer. Finally, ferroelectric hysteresis loops are used to verify that the piezoelectric properties of the PZT thick film are unchanged after the processing of the top electrode.

Keywords PZT · Piezoelectric · Thick film · Top electrode · MEMS device

C. C. Hindrichsen (✉) · T. Pedersen · P. T. Kristiansen · E. V. Thomsen
Department of Micro- and Nanotechnology,
Technical University of Denmark,
2800 Kgs. Lyngby, Denmark
e-mail: christian.hindrichsen@nanotech.dtu.dk

R. Lou-Møller
InSensor A/S, Kvistgaard, Denmark

K. Hansen
Ferroperm Piezoceramics A/S, Kvistgaard, Denmark

1 Introduction

Micro-electromechanical systems (MEMS) utilizing the piezoelectric effect have gained increasing attention [1, 2]. Piezoelectric $Pb(Zr_xTi_{1-x})O_3$ (PZT) thick films have a high coupling factor and show small temperature dependence [3] making them ideal for sensors. Figure 1 shows a schematic drawing of the two MEMS devices of interest, (1) a tri-axial accelerometer, [4, 5] and (2) a piezoelectric Micromachined Ultrasonic Transducer (pMUT) [6, 7]. The two MEMS devices consist of a PZT thick film between a bottom and top electrode on a beam or membrane structure.

The PZT thick film is deposited using screen printing in order to achieve PZT films in the range 10–100 μm [8] which not is possible with sol-gel deposited or sputtered thin films [6, 9, 10]. Thick films result in higher sensitivity [11] and are preferred for some MEMS devices such as accelerometers and pMUT scanner heads. However, screen printed PZT has a rougher surface compared to other deposition techniques due to larger PZT grain sizes which introduces new fabrication challenges with respect to the top electrode formation as most planar processing is optimized for surfaces with a much lower surface roughness. So far most top electrodes on screen printed PZT thick films have been

deposited using screen printing resulting in thickness of approximately 10 μm and maximum lateral resolution around 100 μm [4, 12, 13]. For optimal sensitivity of a MEMS device the top electrode should be as thin as possible, as a thicker top electrode makes a beam or membrane in a MEMS device more stiff. This increase in stiffness decreases the induced strain in the PZT resulting in a lower sensitivity. In an optimal MEMS design the neutral axis of deflection is located in the interface between the bottom electrode and the PZT thick film. The thickness of the bottom electrode is therefore not of concern as the mechanical effect of a thicker bottom electrode can be compensated by making the supporting silicon structure thinner and thereby keeping the neutral axis in the interface. However, the mechanical effect of a thick top electrode can not be compensated and will always have a negative effect on the sensitivity. In conclusion, this motivates for using evaporated top electrodes instead of screen printed top electrodes.

In [14] a top electrode has been sputtered and subsequently pattered with a lift-off process but the process is only briefly described. The purpose of this paper is to investigate the top electrode formation using evaporated thin films for top electrodes with thicknesses of 100–1,000 nm which are more suitable for silicon based MEMS devices.

In this paper screen printed Au and evaporated Al and Pt are tested with the lift-off approach and compared with respect to the deposition process and material properties. The optimal thickness of the evaporated top electrode is found by introducing a roughness factor indicating the change in conductance due to the roughness of the PZT surface.

Due to the rough surface of the PZT film it is preferred to have contact pads next to the PZT thick film on the SiO_2 surface as shown in Fig. 2. This introduced some new challenges as part of the PZT will be in direct contact with the SiO_2 surface not protected by the diffusion barrier layer. A degradation of the piezoelectric properties is seen in the exposed part of the PZT as Si will diffuse into the PZT film [15]. A test structure is used to investigate how local the degradation of the PZT is, by changing the lateral distance L between the top electrode and the exposed PZT.

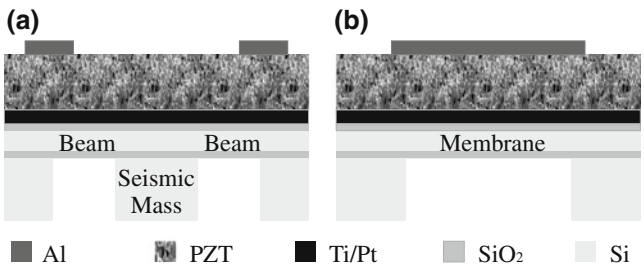

Fig. 1 (**a**) Schematic drawing of an accelerometer with a seismic mass suspended by two beams. (**b**) Schematic of a pMUT with PZT thick film and patterned top and bottom electrode

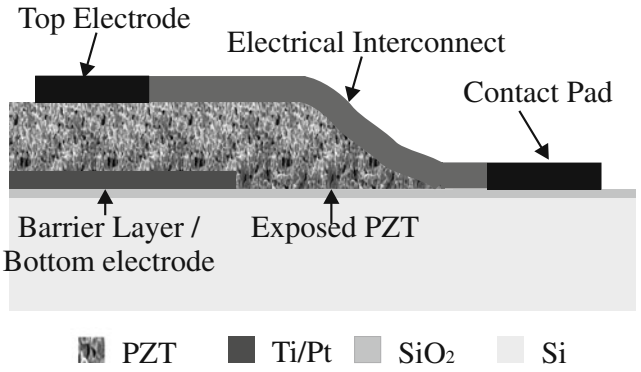

Fig. 2 By introducing the contact pad on the SiO_2 surface part of the PZT thick film will be exposed to the SiO_2 and the piezoelectric properties will be degraded lowering the performance of the MEMS device

Another challenge is to connect the contact pads with the top electrode through a thin film electrical interconnect running down the slope of the PZT thick film.

2 Fabrication

All test structures are fabricated using the same process flow. A 4″ <100> silicon wafer with a 500 nm thick SiO_2 layer is used as substrate material. The bottom electrode, Ti and Pt, is E-beam evaporated with a Wordentec QCL800 Metal Evaporator. The bottom electrode also serves as a diffusion barrier layer during the high temperature sintering between the silicon substrate and the PZT thick film [4, 8]. The PZT powder in an organic vehicle is screen printed through a 77T polyester mesh mask which has 77 lines per inch (30 lines per centimeter). The wires in the mask are 70 μm thick. Subsequently the PZT thick film is sintered at 850°C for one hour. The type of PZT used in this work is the hard doped PZ26 from Ferroperm Piezoceramics A/S [16]. The evaporated top electrode materials, Al or Pt, are patterned with a lift-off technique where metal is evaporated onto a patterned photo resist. Patterning of the top electrode using an etch-back of the metal is challenging as the properties of the PZT typically also are affected [17], thus a lift-off based technique is employed in this work. Acetone is used as a solvent to

remove the photo resist with the unwanted metal on top. Finally the PZT thick film is vertically poled at 150°C with a field of 10 kV/mm for 10 min in order to obtain the piezoelectric properties. The final structure is seen in Fig. 2.

3 PZT surface roughness

Screen printed thick films consist of ceramic grains with grain sizes depending on the fabrication process of the PZT paste. The grain size of the PZT investigated here is approximately 1 μm after sintering and the surface roughness of the thick film is therefore high which induces challenges when depositing the top electrode. The roughness of the surface is divided into a macroscopic roughness due to the mesh used during screen printing and a microscopic roughness due to the grain size of the PZT thick film. The macroscopic roughness is important when considering the performances of the MEMS devices as they are highly dependent on the final thickness of the PZT layer. With respect to the top electrode deposition the microscopic roughness is important as the evaporated metal has to cover the rough PZT thick film surface.

The root mean square value for roughness, R_q, of the screen printed PZT is evaluated with a stylus profiler, Tencor P-1, and to evaluate the microscopic roughness an Atomic Force Microscope (AFM), Dimension 3100 Scanning Probe Microscope, is used.

Figure 3 shows a 800 μm long stylus profiler scan over a 30 μm thick PZT thick film showing the typical macroscopic roughness. The peaks in the scan separated a few hundred micrometers are due to the wires in the polyester mesh mask. The R_q value for the macroscopic roughness is measured to be 1.5 μm based on a scan across the whole wafer. Figure 4 shows a 5 × 5 μm^2 AFM scan of the PZT surface of a 30 μm thick film. The R_q value for the microscopic roughness is found to be 273 nm. The measured macroscopic roughness shows that the thickness of the PZT thick film varies significantly and this variation has to be taken into account for future MEMS devices. The microscopic roughness is higher than for typical PZT thin films and thus it is more difficult to do planar processing on the PZT thick film compared with thin film PZT. For sol gel deposited and sputtered PZT thin films the R_q value is typically below 10 nm [18, 19]. The microscopic roughness shows that the thickness of the evaporated top electrode should be in the order of a few hundred nm in order to get a good coverage.

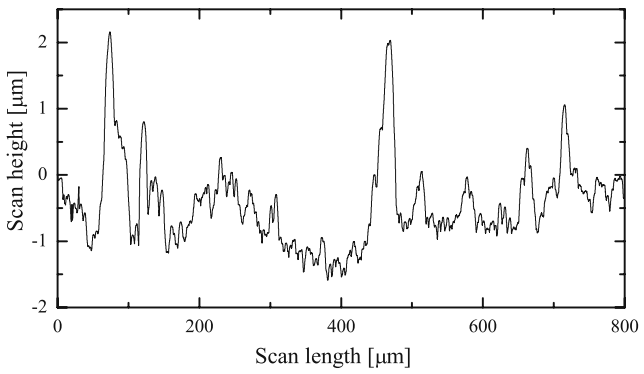

Fig. 3 Stylus profiler scan of a sintered screen printed PZT layer with a thickness of 30 μm showing the macroscopic roughness, R_q, which is found to be 1.5 μm. The peaks show the thickness variation of the PZT thick film caused by the mesh during screen printing

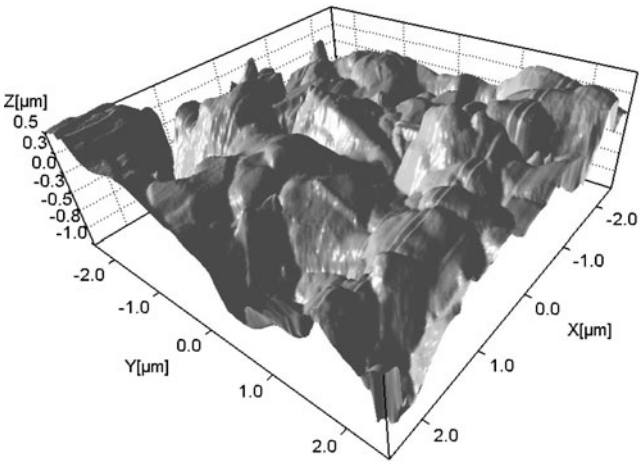

Fig. 4 AFM scan of a 5 × 5 μm^2 area of the 30 μm thick sintered PZT layer giving a microscopic roughness, R_q, of 273 nm

4 Metal deposition techniques

Evaporated top electrodes have the advantages compared to screen printed top electrodes of higher lateral resolution, smaller film thickness, and smaller surface roughness given that that the underlaying surface has a low surface roughness. In this section screen printed top electrodes are compared with evaporated top electrodes patterned with a positive as well as a negative lift-off process.

Deposition of the top electrode is conventionally done by screen printing a gold paste through a 77T polyester mesh mask. Screen printing has a maximum resolution of roughly 100 μm and a metal thickness of 5–10 μm. In Fig. 5 a stylus profiler scan over a screen printed Au wire shows the high thickness of the wire, 7 μm, and the high roughness of the wire.

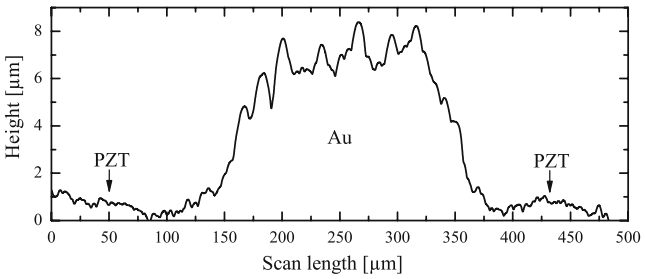

Fig. 5 The roughness of the screen printed top electrode is even greater than the underlying PZT as the stylus profiler scan of a 200 μm wide screenprinted Au electrode shows

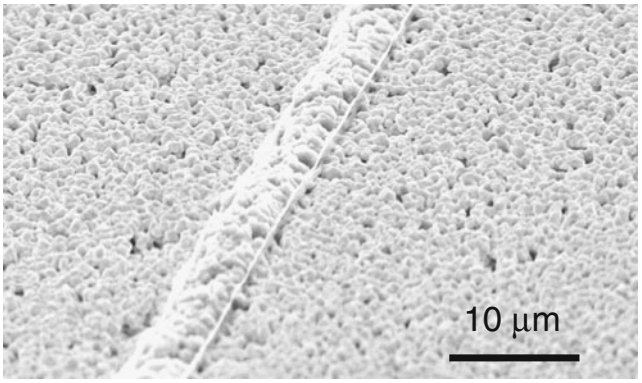

Fig. 7 SEM images of a 1 μm thick Al top electrode on PZT thick film fabricated with a lift-off process. Line widths down to 3 μm and thicknesses down to 100 nm have successfully been fabricated on the rough PZT surface

Lift-off of metal is usually done with a negative photoresist, in this case AZ5214E, due to the inward sloping profile, but can be difficult to control during the spin-on process on the rough PZT surface due to its high viscosity and a maximum thickness of 4.2 μm is obtainable. In this case, the resist has to be thick enough to cover the roughness of the PZT layer. Thus, also a thicker, 9.5 μm, positive photoresist, AZ4562, with a lower viscosity is tested. Previously adhesion problems have been reported when immersing the PZT in photoresist developer (Microposit MF322), resulting in the PZT to peel off [17]. However, in our case the AZ351B developer does not affect the PZT.

For the positive photolithography process the metal covers most of the outward sloped sidewall of the photoresist but there is a small gap for the photo resist solvent, acetone in this case, to penetrate and dissolve the photo resist as seen in Fig. 6. With the positive photolithography process it has been possible to produce 3 μm wide Al wires with a thickness down to 100 nm and a length of 20 mm on the PZT thick film as seen in Fig. 7. The sloped metal sidewalls are not removed by the lift-off process but are easily removed using ultrasonic agitation in the acetone bath, leaving only the metal pattern on the PZT thick film. Ultrasonic agitation can break fragile structures of MEMS devices but have in our investigations not caused any problems.

A direct comparison between a 20 μm wide Pt metal wire processed with the positive and the negative photolithography process is seen in Fig. 8. It is clear that the line definition is better for the wire processed with the positive process. The poor line definition from the negative process is most likely an effect from the coverage problems of the resist because it is too thin compared to the roughness of the PZT.

Pt has a higher melting temperature compared to Al and is therefore more difficult to integrate in a lift-off process as the photo resist is partly hard baked during

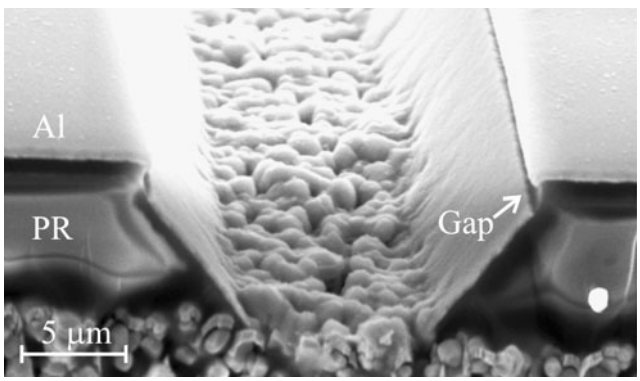

Fig. 6 SEM image of a patterned, positive photoresist (PR) on PZT with 500 nm Al deposited on the photoresist for lift-off. The metal is seen to cover most of the sloped sidewall of the photoresist. However a gap on the sidewalls allows for a lift-off process

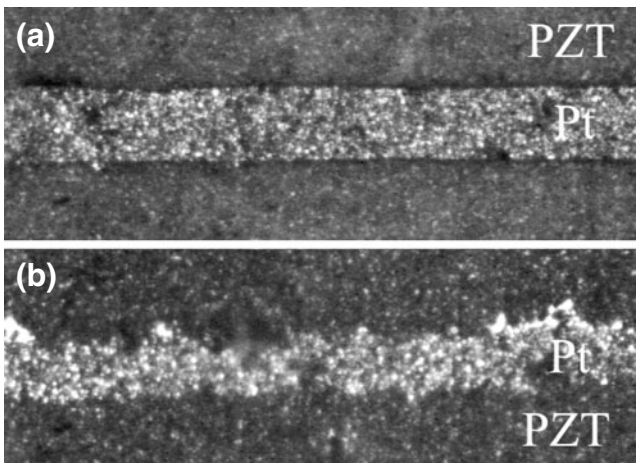

Fig. 8 Comparison of 20 μm wide Pt wires fabricated on PZT with 9.5 μm positive (**a**) and 4.2 μm negative (**b**) photoresist

metal deposition. Al is therefore the preferred metal for an easy lift-off process.

5 Top electrode formations

Three different test structures are applied to investigate the e-beam deposited top electrodes on the screen printed thick film. The first test structure consists of wires of varying widths, w, and thicknesses, h, and is used to investigate how the roughness of the PZT film affects the conductivity of the top electrode. The second test structure investigates the lateral degradation distance of the PZT thick film, L. The final test structure investigates whether it is possible to have well defined and thin electrical interconnects down the slope of the screen printed PZT thick film in order to connect the top electrodes to the contact pads.

5.1 Top electrode thickness

The optimal thickness of the top electrode is a compromise between good conductance and low mechanical influence on device behavior. In order to quantify the conductance of the evaporated top electrode a test mask with wire length, l, ranging 1–20 mm and wire width 3–100 μm are used. The resistance, R, of a wire deposited on the PZT will be greater than the resistance of a similar wire on a flat substrate due to the roughness of the surface. This increase compared with an equivalent wire on a smooth surface relates how the roughness affects the resistance of the top electrode. The resistance of a long and narrow wire on the PZT surface is given by,

$$R = x\frac{\rho l}{wh} \tag{1}$$

where ρ ($\rho_{Al} = 4.41 \times 10^{-8}$ Ωm and $\rho_{Pt} = 1.44 \times 10^{-7}$ Ωm for the evaporated thin films) and h are the resistivity of the metal and the top electrode thickness respectively. The change of resistance due to the roughness of the PZT surface is expressed by the roughness factor x. A roughness factor of one corresponds to a perfect wire on a completely smooth surface. Both Pt and Al are tested as top electrode materials. Wires with thicknesses ranging 100–1,000 nm are deposited. Figure 9 shows the resistance as a function of the inverse wire width for four different thicknesses of Al wires with a length of 5 mm. Each point with respective error bar is based on measurements of four individual wires. Two point probe measurements are performed which result in an offset of the measured resistance due to the contact resistance. The contact resistance

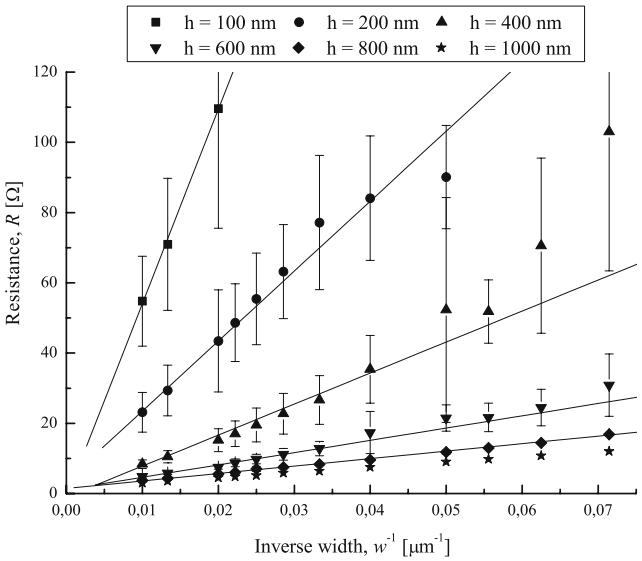

Fig. 9 Resistance as a function of the inverse wire width is shown for different Al top electrode thicknesses, h. A linear, ohmic behavior is seen and the roughness factor is a function of the slope of the linear fits. (l is fixed at 5 mm)

is affected by the surface roughness and the thickness of the metal layer. However, for finding the roughness factor only the slope of the linear fits are of importance and the contact resistance is not of concern. The error of the measured resistance increases for decreasing wire thickness as the effect of the surface roughness of the PZT increases. Similar results are obtained for Pt wires. As the top electrode thickness decreases, the roughness of the PZT has a larger impact on resistance and the roughness factor increases. For increasing top electrode thickness the roughness factor goes asymptotically to one.

The roughness factor is proportional to the slope of the lines in Fig. 9. The roughness factor is decreasing as a function of thickness as seen in Fig. 10. The roughness factor should theoretically be independent of the electrode material although Fig. 10 generally shows a slightly higher value for Pt compared with Al. This is presumably related to the difficulties in the lift-off process of Pt.

The surface roughness of the PZT thick film has proven to have a significant effect on the conductivity of the evaporated top electrodes.

5.2 Lateral degradation distance

The lateral degradation distance is found by placing top electrode pads with increasing distances, L, on a 15 μm PZT thick film. The permittivity of the degraded PZT thick film is decreased dramatically due to diffusion of

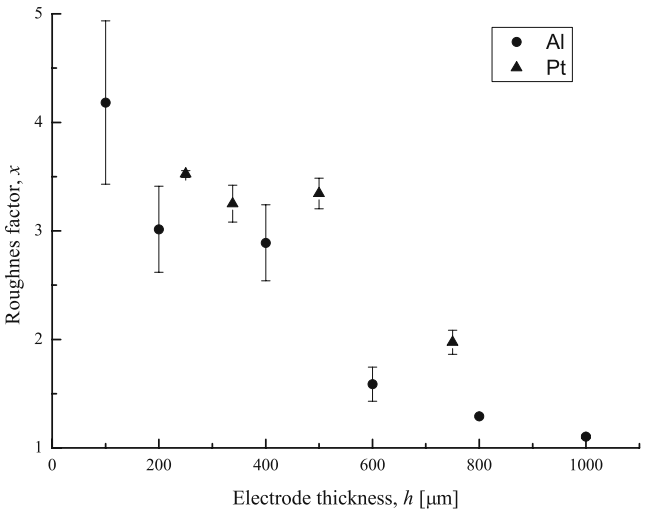

Fig. 10 Roughness factor, x, as a function of metal thickness, h, for thicknesses of 100–1,000 nm

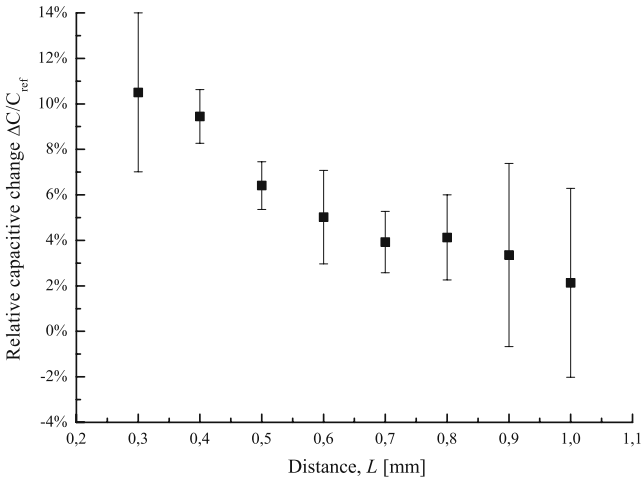

Fig. 12 The relative change in capacitance between top electrode pads and the bottom electrode decreases as the lateral distance L increases. A safety margin $L = 1{,}000$ μm is therefore necessary

Si into the PZT during the sintering process. By measuring the capacitance change between the top electrode pads and the bottom electrode with respect to a reference pad the lateral degradation distance is found. The distance L giving zero change in capacitance equals the lateral degradation level the PZT thick film. Eight top electrode pads width distances L from the edge of the bottom electrode ranging 300–1,000 μm are used to find the necessary safety margin. The pads as well as the reference pad have a size of 500 μm × 2,000 μm. The reference pad is located several cm from the PZT exposed to the SiO_2 surface and its capacitance is measured to be 306 pF corresponding to a relative permittivity of 519. Figure 11 shows a schematic of the test structure seen from the side and from the top respectively.

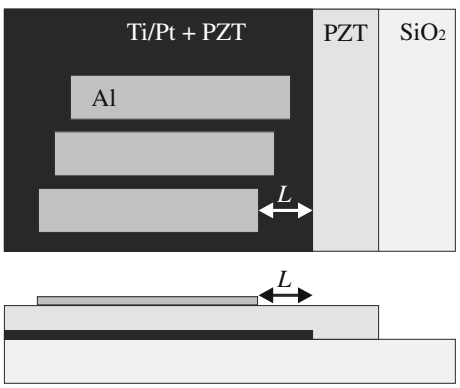

Fig. 11 The figure shows the test structure for measuring the lateral degradation distance seen from the top. It consists of a number of Al pads with varying distance between the edge of the pad and the end of the barrier layer, L

Figure 12 shows the relative change in capacitance between the top electrode pads and the bottom electrode with respect to the reference capacitance as a function of L. The relative change in capacitance is decreasing for increasing L. To avoid degraded piezoelectric properties in the active part of the PZT thick film the top electrode defining the active part should at least be 1,000 μm away from the edge of the bottom electrode.

5.3 Contact pad

It has proven difficult to wire bond to the top electrode on top of the PZT thick film. This is due to the rough surface and the relative soft thick film. It is therefore an advantage to connect the top electrode to contact pads on the smooth SiO_2 surface as shown in Fig. 2. Contact pads on the SiO_2 compared to on PZT have two major advantages. First off all wire bonding is possible and secondly the parasitic capacitance is reduced. In order to connect the top electrode to contact pads on the SiO_2 surface electrical interconnects have to run down the sidewalls of the PZT thick film. Fortunately the sidewalls of the screen printed thick film has a flat slope.

Electrical interconnects with widths down to 15 μm have been fabricated on the slope of the PZT thick film using the positive lift-off process described previously. The height of the PZT thick film for this test structure is 15 μm. Figure 13 shows a SEM image of a electrical interconnect connecting the top electrode on the PZT with the contact pad on the SiO_2 surface.

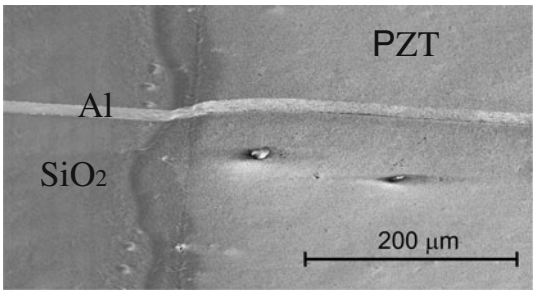

Fig. 13 A SEM image of a 15 µm wide Al electrical interconnect down the slope of the screen printed PZT thick film (*right*) making it possible to connect the top electrode to a contact pad located on the SiO_2 surface

5.4 Piezoelectric properties

For the MEMS applications shown in Fig. 1 it is important that the piezoelectric properties do not degrade during the processing of the top electrodes. During processing the PZT thick film is exposed to photo resist, a photolithographic developer and acetone as solvent.

In order to investigate the influence of the top electrode processing on the performance of the PZT thick film, ferroelectric hysteresis loops were recorded. A ferroelectric hysteresis loop of the PZT on a silicon substrate with evaporated top electrodes is compared to a reference PZT thick film deposited on alumina with a screen printed top electrode. The results displayed in Fig. 14 show a slight difference in the hysteresis loops of PZT thick film deposited on alumina and silicon respectively. The two loops are misaligned along the polarization axis, but the average remnant polarization of the two are the same. There is however, a slight difference in coercive field which can be due to a difference in mechanical and chemical properties of the substrate materials. An investigation of the exact mechanism behind this is however, beyond the scope of this paper. Based on the similarities of the remnant polarization we conclude that the performance of the thick film is not impaired. A comparison of the properties of PZT thick film with a bulk PZT material is done in [8].

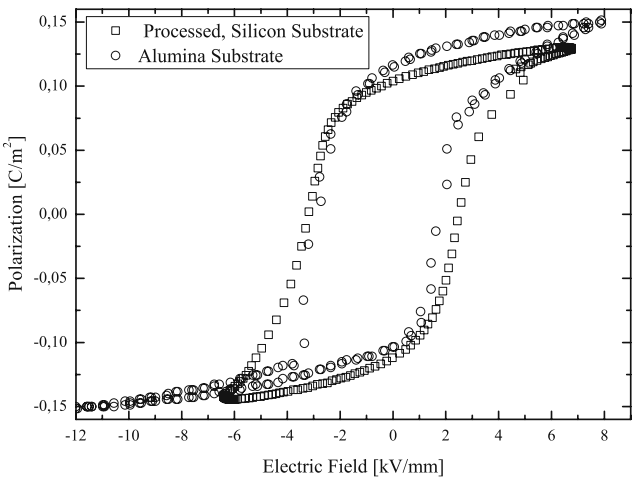

Fig. 14 The plot shows ferroelectric hysteresis loops for the PZT thick film on a silicon substrate after the top electrode lift off process and for reference a PZT thick film on a Alumina substrate with a screen printed top electrode. The similarity of the two loops proves that the piezoelectric properties of the PZT thick film are not degraded during the processing steps

Appendix A shows the elasticity coefficients, [*S*], the piezoelectric charge coefficients, [*d*] and the piezoelectric voltage coefficients, [*g*] for the PZT thick film.

6 Discussion

The results from the test structures show that the top electrode can be deposited using e-beam evaporated metals and patterned with a lift-off process. This gives higher lateral resolution compared to screen printed top electrodes and therefore better device performance.

As demonstrated, the resistance of wires deposited on PZT is not simply linearly dependent on metal thickness due to the roughness of the PZT. This aspect has to be considered when designing PZT thick film based devices. A top electrode thickness of several hundred nm seems very high compared to what have been presented previously [9] but as Fig. 10 shows, the high surface roughness demands top electrodes in this thickness range. As long as the top electrode is deposited after the sintering process almost all metals are candidates.

At first Al seems to be preferable compared with Pt due to the lower Young's modulus, lower processing temperature and less influence on the mechanical behavior. For piezoelectric MEMS devices with a sandwich structure of different layers (see Fig. 1) the coefficients of thermal expansion, CTE, should also be considered. Al and Pt have 24 µm/(m°C) and 9.2 µm/(m°C) respectively and Si and PZT have 2.6 µm/(m°C) and 2.0 µm/(m°C), respectively [20]. Considering the CTE, Pt is the preferred choice.

The option with a electrical interconnect down the slope of the PZT thick film also allows to connect different top electrodes using electrical interconnects on the SiO_2 which is useful for MEMS applications. A drawback of having the contact pads on the SiO_2 surface is the necessary safety margin of at least 1,000 µm which increases chip size significantly.

A way to avoid this safety margin could be by introducing a insulating barrier layer between the SiO_2 and the PZT thick film. Several candidates such as ZrO_2 [6], Al_2O_3 [21] and PbO [22] have been proposed but none have so far been shown functional for PZT thick films on Si substrates sintered at 850°C.

7 Conclusion

It has proven possible to integrate screen printing of PZT thick films on silicon substrates. E-beam evaporation of top electrodes subsequently patterned with a positive lift-off process has proven to have higher lateral resolution and less mechanical influence due to thinner films on the potential MEMS devices compared to screen printed top electrodes. The roughness of the PZT thick film has a significant effect on the conductance of the top electrode and a 100 nm thick top electrode has a 4.5 times higher resistivity compared to a similar wire on a planar surface. In order to make the MEMS devices compatible with mainstream silicon contacting and packaging schemes a structure with contact pads on the planar silicon substrate instead of on the rougher PZT surface was presented. Such a structure exposes part of the PZT thick film to the silicon substrate resulting in a degradation of the piezoelectric properties of the PZT thick film up to 1,000 μm away. For contacting the top electrode on the PZT thick film with the contact pad on the silicon surface a electrical interconnect was successfully patterned down the slope of the PZT thick film.

It is believed that evaporated thin films subsequently patterned with a lift-off process is the most suitable process for realizing top electrode with high lateral resolution and a minimum of mechanical influence on the MEMS device.

Appendix A

The PZT thick film have the following properties, where $[S]$ is compliance coefficient, $[d]$ is the piezoelectric charge coefficient and $[g]$ is the piezoelectric voltage coefficient. The coefficients are provided by Ferroperm Piezoceramics A/S.

$$[S] = \begin{bmatrix} 16 & -5.3 & -7.2 & 0 & 0 & 0 \\ -5.3 & 16 & -7.2 & 0 & 0 & 0 \\ -7.2 & -7.2 & 23 & 0 & 0 & 0 \\ 0 & 0 & 0 & 60 & 0 & 0 \\ 0 & 0 & 0 & 0 & 60 & 0 \\ 0 & 0 & 0 & 0 & 0 & 42.6 \end{bmatrix} \times 10^{-12} \frac{\mathrm{m}^2}{\mathrm{N}}$$

$$[d] = \begin{bmatrix} 0 & 0 & 0 & 0 & 300 & 0 \\ 0 & 0 & 0 & 300 & 0 & 0 \\ -51 & -51 & 168 & 0 & 0 & 0 \end{bmatrix} \times 10^{-12} \frac{\mathrm{C}}{\mathrm{N}}$$

$$[g] = \begin{bmatrix} 0 & 0 & 0 & 0 & 53 & 0 \\ 0 & 0 & 0 & 53 & 0 & 0 \\ -9 & -9 & 39 & 0 & 0 & 0 \end{bmatrix} \times 10^{-3} \frac{\mathrm{Vm}}{\mathrm{N}}$$

References

1. S. Trolier-Mckinstry, P. Muralt, Thin film piezoelectrics for MEMS. J. Electroceramics **12**, 7–17 (2004)
2. R.A. Dorey, R.W. Whatmore, Electroceramic thick film fabrication for MEMS. J. Electroceramics **12**, 19–32 (2004)
3. G.H. Gautschi, *Piezoelectric Sensorics* (Springer, 2002)
4. S.P. Beeby, N.J. Grabham, N.M. White, Microprocessor implemented self-validation of thick-film PZT/silicon accelerometer. Sens. Actuators A **92**, 168–174 (2001)
5. C.C. Hindrichsen, E.V. Thomsen, R. Lou-Møller, T. Bove, in MEMS Accelerometer with Screen Printed Piezoelectric Thick Film. 5th IEEE Conference on Sensors, Daegu, South Korea (2007), pp. 1477–1480
6. F.F.C. Duval, R.A. Dorey, R.W. Wright, Z. Huang, R.W. Whatmore, Fabrication and modeling of high-frequency PZT composite thick film membrane resonators. IEEE Trans. Ultrason. **51**, 1255–1261 (2004)
7. P. Maréchal, F. Levassort, J. Holc, L.-P. Tran-Huu-Hue, M. Kosec, M. Lethiecq, High-frequency transducers based on integrated piezoelectric thick films for medical imaging. IEEE Trans. Ultrason. Ferroelectr. Freq. Control **53**, 1524–1533 (2006)
8. R. Lou-Møller, C.C. Hindrichsen, L.H. Thamprup, T. Bove, E. Ringgaard, A.F. Pedersen, E.V. Thomsen, Screen-printed piezoceramics thick films for miniaturised devices. J. Electroceramics **19**, 333–338 (2007)
9. Z. Wang, W. Zhu, J. Miao, H. Zhu, C. Chao, O.K. Tan, Micromachined thick film piezoelectric ultrasonic transducers array. Sens. Actuators A **130–131**, 485–490 (2006)
10. L. Wang, R.A. Wolf Jr., Y. Wang, K.K. Deng, L. Zou, R.J. Davis, S. Troiler-McKinstry, Design, fabrication, and measurement of high-sensitivity piezoelectric microelectromechanical systems accelerometers. J. Microelectromechanical Syst. **12**(4), 433–439 (2003)
11. Y. Jeon, Y.G. Seo, S.J. Kim, K. No, Integr. Ferroelectr. **30**, 91–101 (2000)
12. L. Simon, S. Le Dren, PZT and PT screen-printed thick films. J. Eur. Ceram. Soc. **21**, 1441–1444 (2001)
13. C. Lucat, F. Menil, R. Von Der Muhll, Thick-film densification for pyroelctric sensors. Meas. Sci. Technol. **8**, 38–41 (1997)
14. H.J. Kim, Y-B. Kim, J-Y. Kang, T.S. Kim, Fabrication of resonant behavior of PZT thick film cantilever for BioChip. Integr. Ferroelectr. **50**, 11–20 (2002)
15. R. Maas, M. Koch, N.R. Harris, N.M. White, A.G.R. Evans, Thick-film printing of PZT onto silicon. Mater. Lett. **31**, 109–112 (1997)
16. Company homepage: www.ferroperm-piezo.com
17. S.P. Beeby, A. Blackburn, N.M. White, Processing of PZT piezoelectric thick films on silicon for microelectromechani-

cal systems. J. Micromechanics Microengineering **9**, 218–229 (1999)
18. X.G. Tang, Q.X. Liu, L.L. Jiang, A.L. Ding, Optical properties of $Pb(Zr_xTi_{1-x})O_3$ (x = 0.4, 0.6) thin films on Pt-coated Si substrates studied by spectroscopic ellipsometry. Mater. Chem. Phys. **103**(2–3), 329–333 (2007)
19. O. Blanco, J. Heiras, J.M. Siqueiros, E. Martinez, A.G. Castellanos-Guzman, PZT films grown by RF sputtering at high oxygen pressure. J. Mater. Sci. Lett. **22**, 449–453 (2003)
20. D.R. Lide, *Handbook of Chemistry and Physics*, 73rd edn. (CRC Press, Boca Raton, FL, 1993)
21. M. Hrowat, J. Holc, S. Drnovsek, D. Belavic, J. Cilensek, M. Kosec, PZT thick films on LTCC substractes with an interposed alumina barrier layer. J. Eur. Ceram. Soc. **26**, 897–900 (2006)
22. C. Park, M. Won, Y. Oh, Y. Son, An XPS study and electrical properties of $Pb_{1.1}Zr_{0.53}Ti_{0.47}O_3$/PbO/Si (MFIS) structures according to the substarte temperature of PbO buffer layer. Appl. Surf. Sci. **252**, 1988–1997 (2005)